

Chapter 4

An innovative Vieta-Fibonacci wavelet collocation method for the numerical solution of three-component Brusselator reaction diffusion system of fractional order

4.1 Introduction

There are many kinds of fractional derivatives viz., Riemann-Liouville fractional derivative [22], Caputo fractional derivative [22], Atangana-Baleanu derivative [90], M-truncate derivative [91], Beta-fractional derivative and [92, 93] etc. These fractional derivatives and integrals help us to understand and describe the complex behaviors in many real-world systems. The significance of fractional calculus lies in its ability to model the things which don't behave in a standard way. For example, it helps us study how certain materials stretch and deform, how some substances diffuse in unusual patterns, and how signals in communication systems can be processed more effectively. By using fractional calculus, the scientists and engineers can better understand these phenomena and also design better control systems, improve image processing, and optimize various processes. It opens up new possibilities to explore and solve problems in different fields, making it an invaluable tool in modern science and technology. As we delve deeper into fractional calculus theory, we

unlock a better understanding of the hidden complexities that surround us.

The applications of fractional differential equations are quite diverse and can be found in various fields such as Diffusion and Transport [94], Viscoelasticity [95], Electrical Circuits [96] etc. Several numerical methods can be found in literature such as in [97] the Homotopy perturbation method has been used for the approximate numerical solution of time fractional Lotka-Volterra equation, in [98] a class of coupled fractional order PDEs has been approximated based on operational matrices(OM) of fractional order integrations and differentiations, in [99] the Laplace optimization decomposition method has been proposed to obtain the approximate solution of the nonlinear FPDEs with the fractional derivative. The modified power series solution method with conformable derivatives was used by [100] to solve a coupled system of nonlinear FPDEs, [101] has proposed a method for solving nonlinear FDE with finite difference methods based on nonuniform meshes, [102] has used the shifted Jacobi collocation method to solve fractional nonlinear cable equations in one and two-dimensional spaces. A spectral numerical approach has been presented by [53] for solving fractional diffusion-wave equations and fractional wave equations of second, fourth-order. In [103] the power series method is used for the numerical simulation of non-integer differential equation, an approach has been developed in [104] that examines fractional-order shock wave equations and wave equations associated with gas motion, [60] has used Variational iteration method for analytical approximate solution of a fractional diffusion equation, [105] has solved system of FPDE using Optimization technique, [106] has solved third kind Volterra integral equation, [107] has used the spectral Galerkin technique for the computation of time fractional delay differential and PDEs etc.

The three-component Brusselator reaction-diffusion system is a mathematical model

that describes the dynamics of a chemical reaction involving three components. It is an extension of the original Brusselator model, which was proposed by Ilya Prigogine and Robert Lefever in the context of nonlinear chemical kinetics. The fractional version of the three-component Brusselator reaction-diffusion system can be written in the following way [108] as

$$\begin{aligned}\frac{\partial^\alpha u}{\partial t^\alpha} &= d_1 \frac{\partial^2 u}{\partial x^2} + a_1 - (b_1 + w)u + u^2 v + f_1(x, t), \\ \frac{\partial^\alpha v}{\partial t^\alpha} &= d_2 \frac{\partial^2 v}{\partial x^2} + uw - u^2 v + f_2(x, t), \quad (x, t) \in [0, 1] \\ \frac{\partial^\alpha w}{\partial t^\alpha} &= d_3 \frac{\partial^2 w}{\partial x^2} - uw + c_1 + f_3(x, t),\end{aligned}\tag{4.1}$$

where d_1, d_2 and d_3 are diffusion coefficients, the concentration of two intermediary reactants are represented by $u(x, t)$ and $v(x, t)$ while concentration of input concentration is denoted by $w(x, t)$ and a_1, b_1 and c_1 denote the rate constants. The Brusselator reaction-diffusion system finds applications in various fields due to its ability to model pattern formation and complex behavior in dynamic systems such as the Brusselator model is used in chemical kinetics to study the behavior of autocatalytic reactions, where a substance catalyzes its own production. It helps to understand the formation of intricate chemical patterns observed in certain reactions.

In this chapter, a computational strategy has been suggested based on the collocation method and the operational matrices of the Vieta-Fibonacci wavelet. The primary points are as follows:

- The goal of this chapter is to construct the operational matrices of integer as well as Caputo fractional order derivative based on the Vieta-Fibonacci wavelets for the first time for solving the three-component Brusselator reaction-diffusion system of fractional order arising in chemical reactions.

- The existence, uniqueness of the solution, and Ulam-Hyers stability of the model are discussed.
- Theoretical discussion on the error bound and convergence analysis for the proposed method has been presented.
- The efficiency and accuracy of the suggested technique are confirmed through an error analysis between the obtained numerical results and the existing analytical results for the particular forms of the considered model.

The combination of wavelet OM and collocation method provides an efficient and accurate numerical approach for solving FPDEs. Its ability to handle fractional derivatives, adaptively refine the spatial grid, and provide accurate approximations makes it a valuable tool for modeling and simulating complex systems even in fractional order system. Some available wavelet methods are as follows: [109] has derived generalized Taylor wavelet method for the numerical investigation of distributed order fractional PDE, [110] has developed Haar wavelet and collocation method for the numerical solution of system of fractional ODE, [111] has investigated modified version of Hermite wavelet for the simulation of space-time fractional PDE, [112] has used Chebyshev wavelet method for fractional-order Volterra-Fredholm integro-differential equations. Based on two-dimensional Müntz-Legendre hybrid functions, [113] has proposed a numerical method for solving FPDEs. The article [114] has developed a method for FPDEs based on the generalized Gegenbauer-Humbert wavelets and their OM. The article [115] has used Legendre wavelet for solving ODE and FPDE respectively, while [116] has presented Bernoulli wavelet for PDEs.

4.2 Vieta-Fibonacci wavelets

Theorem 4.1. Let $VF_n^*(x)$ be the Vieta-Fibonacci polynomials that are shifted into $[0, 1]$, then we have

$$\frac{d}{dx}[VF_n^*(x)] = \sum_{\substack{k=0 \\ (k+n) \text{ odd}}}^{n-1} 4k VF_k^*(x). \quad (4.2)$$

Proof. Expanding the function $f(x)$ in terms of VF polynomials in the following way

$$f(x) = \sum_{k=0}^{\infty} \hat{c}_k VF_k(x). \quad (4.3)$$

Now, differentiating both sides w.r. to x , we have

$$f'(x) = \sum_{k=0}^{\infty} \hat{c}_k^{(1)} VF_k(x), \quad (4.4)$$

where

$$\hat{c}_k^{(1)} = k \sum_{\substack{p=1+k \\ (k+p) \text{ odd}}}^{\infty} \hat{c}_p, \quad k \geq 0. \quad (4.5)$$

Now, assuming $f(x) = VF_n(x)$ in Eq.(4.3), we obtain $\hat{c}_n = 1$ and $\hat{c}_n = 0$ for $i \neq n$, consequently

$$\hat{c}_k^{(1)} = \begin{cases} k, & (n+k) \text{ is odd, } k \leq n-1, \\ 0, & \text{otherwise.} \end{cases}$$

The following required expression is obtained using $\hat{c}_k^{(1)}$ in Eq.(4.4) as

$$\frac{d}{dx}[VF_n(x)] = \sum_{\substack{k=0 \\ (k+n) \text{ odd}}}^{n-1} k VF_k(x). \quad (4.6)$$

Substituting $4x - 2 = t$ in Eq.(4.6), we get

$$\frac{d}{dx}[VF_n^*(x)] = \sum_{\substack{k=0 \\ (k+n) \text{ odd}}}^{n-1} 4k VF_k^*(x).$$

□

4.2.1 Vieta-Fibonacci wavelets

Vieta-Fibonacci wavelets are constructed from Vieta-Fibonacci polynomials. Vieta-Fibonacci wavelets $\psi_{n,m}(t) = \psi(k, n, m, t)$ have four arguments with $n = 0, 1, 2, \dots, 2^k - 1$, $k \in \mathbb{N} \cup \{0\}$, and m is the degree of polynomial and t is normalized time. Vieta-Fibonacci wavelets are defined on the interval $[0, 1]$ as [117]

$$\psi_{n,m}(x) = \begin{cases} 2^{\frac{k}{2}} \sqrt{\frac{8}{\pi}} VF_m^*(2^k x - n), & x \in \left[\frac{n}{2^k}, \frac{n+1}{2^k}\right], \\ 0, & \text{otherwise,} \end{cases} \quad (4.7)$$

where $m = 1, 2, 3, \dots, M$.

VF Wavelets are orthogonal on the interval $\left[\frac{n}{2^k}, \frac{n+1}{2^k}\right]$ w.r.to the weight function $\omega_n(x)$ i.e.,

$$\int_{\frac{n}{2^k}}^{\frac{n+1}{2^k}} \psi_{nm}(x) \psi_{n'm'}(x) \omega_n(x) dx = \begin{cases} \frac{\pi^2}{64}, & n = n' \text{ and } m = m', \\ 0, & \text{otherwise,} \end{cases} \quad (4.8)$$

where

$$\omega_n(x) = w(2^k x - n) = \begin{cases} \sqrt{(2^k x - n) - (2^k x - n)^2}, & x \in \left[\frac{n}{2^k}, \frac{n+1}{2^k}\right], \\ 0, & \text{otherwise.} \end{cases}$$

If $f(x)$ is a function defined over the interval $[0, 1]$, then we can write $f(x)$ as the combination of Vieta-Fibonacci wavelets as

$$f(x) = \sum_{n=0}^{\infty} \sum_{m=0}^{\infty} c_{nm} \psi_{n,m}(x), \quad (4.9)$$

where $c_{nm} = \int_0^1 f(x) \psi_{n,m}(x) \omega_n(x) dx$.

Now, this infinite series is truncated as follows:

$$f(x) = \sum_{n=0}^{2^k-1} \sum_{m=1}^M c_{nm} \psi_{n,m}(x) \cong C^T \Psi(x), \quad (4.10)$$

where C and $\Psi(x)$ are column vectors of order $2^k M$ and given by

$$C = [c_{01}, c_{02} \cdots c_{0M} | c_{11}, c_{12} \cdots c_{1M} | \cdots | c_{2^k-1, 1}, c_{2^k-1, 2} \cdots c_{2^k-1, M}]^T, \quad (4.11)$$

and

$$\Psi(x) = [\psi_{01}, \psi_{02} \cdots \psi_{0M} | \psi_{11}, \psi_{12} \cdots \psi_{1M} | \cdots | \psi_{2^k-1, 1}, \psi_{2^k-1, 2} \cdots \psi_{2^k-1, M}]^T. \quad (4.12)$$

4.3 Derivation of VF wavelet OM

In this section, the OM of the derivative of VF wavelets for both integer and fractional order derivatives have been derived.

4.3.1 OM of integer order derivative

Theorem 4.2. Let $\Psi(x)$ be the VF wavelets defined in Eq.(4.12), then the derivative of $\Psi(x)$ will be

$$\frac{d\Psi(x)}{dx} = D\Psi(x), \quad (4.13)$$

where D is the derivative matrix of order \hat{m} ($\hat{m} = 2^k M$) and is given by

$$D = \text{diag}(F, F, \dots, F), \quad (4.14)$$

where F is a square matrix of order M , whose elements are calculated as

$$F_{p,q} = \begin{cases} 2^{k+2}q, & p = 2, \dots, M, \quad q = 1, \dots, (p-1) \text{ and } (p+q) \text{ odd} \\ 0, & \text{otherwise.} \end{cases} \quad (4.15)$$

Proof. With the help of VF polynomial shifted into $[0, 1]$, the p th element of the vector $\Psi(x)$ is given by

$$\Psi_p(x) = \psi_{n,m} = 2^{\frac{k}{2}} \sqrt{\frac{8}{\pi}} VF_m^*(2^k x - n) \chi_{[\frac{n}{2^k}, \frac{n+1}{2^k}]}, \quad (4.16)$$

where $p = nM + m$, $n = 0, 1, \dots, (2^k - 1)$, $m = 1, 2, \dots, M$, $\chi_{[\frac{n}{2^k}, \frac{n+1}{2^k}]}$ is the characteristic function.

Differentiating Eq.(4.16) w.r. to x , we get

$$\frac{d\Psi_p(x)}{dx} = 2^{\frac{3k}{2}} \sqrt{\frac{8}{\pi}} VF_m'(2^k x - n) \chi_{[\frac{n}{2^k}, \frac{n+1}{2^k}]}. \quad (4.17)$$

Since it is zero outside the interval $[\frac{n}{2^k}, \frac{n+1}{2^k}]$, therefore $\frac{d\Psi_p(x)}{dx} = 0$ for $p = 1, M + 1, 2M + 1, \dots, (2^k - 1)M + 1$.

Now, substituting the value of $VF_m^*(2^k x - n)$ in Eq.(4.17) from Theorem 4.1, we obtain

$$\frac{d\Psi_p(x)}{dx} = 2^{\frac{3k}{2}} \sqrt{\frac{8}{\pi}} \sum_{\substack{j=0 \\ (m+j) \text{ odd}}}^{m-1} 4j VF_j^*(2^k x - n) \chi_{[\frac{n}{2^k}, \frac{n+1}{2^k}]}. \quad (4.18)$$

Expanding the above equation in VF wavelets, we have

$$\frac{d\Psi_p(x)}{dx} = 2^{\frac{3k}{2}} \sqrt{\frac{8}{\pi}} \sum_{\substack{j=0 \\ (m+j) \text{ odd}}}^{m-1} 4j VF_j^*(2^k x - n) \chi_{[\frac{n}{2^k}, \frac{n+1}{2^k}]} = 2^k \sum_{\substack{q=0 \\ (p+q) \text{ odd}}}^{p-1} 4q \Psi_{nM+q}(x). \quad (4.19)$$

If we choose $F_{p,q}$ as

$$F_{p,q} = \begin{cases} 2^{k+2}q, & p = 2, \dots, M, \quad q = 1, \dots, (p-1) \text{ and } (p+q) \text{ odd,} \\ 0, & \text{otherwise,} \end{cases}$$

then the required result is obtained. \square

Remark The operational matrix for the n th derivative may be obtained by applying Eq.(4.13) as

$$\frac{d^n \Psi(x)}{dx^n} = D^n \Psi(x),$$

where D^n is the n th power of matrix D and n is some positive integer.

4.3.2 OM of fractional order derivative

Theorem 4.3. Let $\Psi(x)$ be the VF wavelet vector as defined in Eq.(4.12) on the interval $[\frac{n}{2^k}, \frac{n+1}{2^k}]$ and ${}_0^c D_x^\alpha \psi_{nm}(x)$ be the fractional derivative of VF wavelets in Caputo

sense of order $\alpha > 0$ ($[\alpha] - 1 < \alpha < [\alpha]$) then for $k = 0$, we have

$${}_0^c D_x^\alpha \psi_{nm}(x) = \begin{cases} \sum_{j=1}^M \Omega_\alpha^{(n)}(m, j) \psi_{nj}(x), & m \geq [\alpha], \\ 0, & 0 \leq m < [\alpha], \end{cases} \quad (4.20)$$

where

$$\begin{aligned} \Omega_\alpha^{(n)}(m, j) &= \sum_{i=[\alpha]}^m \frac{(-1)^{-i+j+m} 2^{2+2i+k\alpha} j! \Gamma(1+i+m) \Gamma(\frac{3}{2}+i-\alpha)}{\sqrt{\pi} \Gamma(2+2i)} \\ &\times \frac{\text{HypergeometricPFQ}[\{1-j, 1+j, \frac{3}{2}+i-\alpha\}, \{\frac{3}{2}, 3+i-\alpha\}, 1]}{\Gamma(m-i)\Gamma(i+1-\alpha)\Gamma(3+i-\alpha)}. \end{aligned}$$

Proof. If $m < [\alpha]$, then there is nothing to prove; therefore, let us assume that $m \geq [\alpha]$, we have

$$\psi_{nm}(x) = 2^{k/2} \sqrt{\frac{8}{\pi}} \sum_{i=1}^m b_{mi} (2^k x - n)^i \chi_{I_{nk}(x)}, \quad (4.21)$$

where $I_{nk}(x) = [n/2^k, (n+1)/2^k]$, $n = 0, 1, \dots, 2^k - 1$, $m = 1, 2, \dots, M$. Now applying the Caputo fractional derivative to both sides of the above equation, we get

$${}_0^c D_x^\alpha \psi_{nm}(x) = \sum_{i=1}^m a_{mi} {}_0^c D_x^\alpha \left(x - \frac{n}{2^k}\right)^i \chi_{I_{nk}(x)} = \sum_{i=[\alpha]}^m \frac{a_{mi}(i)!}{\Gamma(1+i-\alpha)} (x - n/2^k)^{i-\alpha} \chi_{I_{nk}(x)}, \quad (4.22)$$

where $a_{mi} = 2^{(1/2+i)k} \sqrt{\frac{8}{\pi}} b_{mi}$ and $b_{mi} = \frac{(-1)^{m-i-1} 2^{2i} \Gamma(m+i+1)}{\Gamma(m-i)\Gamma(2i+2)}$.

The VF wavelets expansion of this function is limited to only those components which are non-zero at the time of this distribution because the value of $(x - n/2^k)^{i-\alpha} \chi_{I_{nk}(x)}$ outside this interval $[n/2^k, (n+1)/2^k]$ is a zero value. Therefore, the VF wavelets

expansion of this function gives

$$(x - n/2^k)^{i-\alpha} \chi_{I_{nk}(x)} = \sum_{j=1}^M \psi_{nj}(x) e_{ij}, \quad i = [\alpha], [\alpha] + 1, \dots, m, \quad (4.23)$$

where

$$\begin{aligned} e_{ij} &= \int_{n/2^k}^{(n+1)/2^k} (x - n/2^k)^{i-\alpha} \psi_{nj}(x) \omega_n(x) dx = \sum_{r=0}^j c_{jr} \int_{n/2^k}^{(n+1)/2^k} (2^k x - n)^{r-\alpha+i} \omega_n(x) dx, \\ &= \sum_{r=0}^j \frac{c_{jr} \sqrt{\pi} \Gamma(\frac{3}{2} + r + i - \alpha)}{2^{k+1} \Gamma(3 + r + i - \alpha)}, \end{aligned} \quad (4.24)$$

where

$$c_{jr} = \frac{2^{\frac{k}{2}} \sqrt{\frac{8}{\pi}}}{2^{(i-\alpha)k}} b_{jr}.$$

Substituting Eqs.(4.23) – (4.24) into Eq.(4.22), we get

$${}_0^c D_x^\alpha \psi_{nm}(x) = \sum_{j=1}^M \Omega_\alpha^{(n)}(m, j) \psi_{nj}(x), \quad (4.25)$$

where $\Omega_\alpha^{(n)}(m, j) = \sum_{i=[\alpha]}^m \Theta_{mji}$ and Θ_{mji} is given by

$$\Theta_{mji} = \frac{a_{mi}(i)!}{\Gamma(1 - \alpha + i)} \times \sum_{r=0}^j \frac{c_{jr} \sqrt{\pi} \Gamma(\frac{3}{2} + r + i - \alpha)}{2^{k+1} \Gamma(3 + r + i - \alpha)}.$$

After performing mathematical calculation, $\Omega_\alpha^{(n)}(m, j)$ can be written as

$$\begin{aligned} \Omega_\alpha^{(n)}(m, j) &= \sum_{i=[\alpha]}^m \frac{(-1)^{-i+j+m} 2^{2+2i+k\alpha} j! \Gamma(1 + i + m) \Gamma(\frac{3}{2} + i - \alpha)}{\sqrt{\pi} \Gamma(2 + 2i)} \\ &\times \frac{\text{HypergeometricPFQ}[\{1 - j, 1 + j, \frac{3}{2} + i - \alpha\}, \{\frac{3}{2}, 3 + i - \alpha\}, 1]}{\Gamma(m - i) \Gamma(i + 1 - \alpha) \Gamma(3 + i - \alpha)}, \end{aligned}$$

where HypergeometricPFQ is the Generalized hypergeometric function.

Now, Eq.(4.25) will be

$${}^c_0D_x^\alpha \psi_{nm}(x) = [\Omega_\alpha^{(n)}(m, 1), \Omega_\alpha^{(n)}(m, 2), \dots, \Omega_\alpha^{(n)}(m, M)] \Psi_n(x). \quad (4.26)$$

The proof is now completed. \square

Theorem 4.4. Let $\Psi(x)$ be the VF wavelet vector as defined in Eq.(4.12) on the interval $[\frac{n}{2^k}, \frac{n+1}{2^k}]$ and ${}^c_0D_x^\alpha \Psi(x)$ be the fractional derivative of VF wavelets in Caputo sense of order $\alpha > 0$ ($[\alpha] - 1 < \alpha < [\alpha]$), then for $k = 0$, we have

$${}^c_0D_x^\alpha \Psi(x) \simeq B^\alpha \Psi(x) \quad (4.27)$$

where B^α is VF wavelet OM of order $\hat{m} \times \hat{m}$ and is given by

$$B^\alpha = \begin{pmatrix} 0 & 0 & \dots & 0 \\ \vdots & \vdots & \dots & \vdots \\ \Omega_\alpha^{(n)}([\alpha], 1) & \Omega_\alpha^{(n)}([\alpha], 2) & \dots & \Omega_\alpha^{(n)}([\alpha], M) \\ \Omega_\alpha^{(n)}([\alpha] + 1, 1) & \Omega_\alpha^{(n)}([\alpha] + 1, 2) & \dots & \Omega_\alpha^{(n)}([\alpha] + 1, M) \\ \vdots & \vdots & \dots & \vdots \\ \Omega_\alpha^{(n)}(M, 1) & \Omega_\alpha^{(n)}(M, 2) & \dots & \Omega_\alpha^{(n)}(M, M) \end{pmatrix},$$

Proof. Using Theorem 4.3, the proof can be done easily. \square

4.4 Existence, uniqueness, and stability results

The purposes of this section is to provide the mathematical analysis of the presented model. First, the existence and uniqueness of the solution of the discussed

model are demonstrated and then the Ulam-Hyers stability of the model is discussed.

4.4.1 Existence and uniqueness

Consider the fractional order three-component time fractional order Brusselator reaction diffusion model as given in Eq.(4.1).

Now, introducing the Riemann-Liouville integral operator of fractional order in Eq.(4.1), we have

$$\begin{aligned} u(x, t) - u(x, 0) &= I_t^\alpha \left(d_1 u_{xx} + a_1 - (b_1 + w)u + u^2 v + f_1(x, t) \right), \\ &= \frac{1}{\Gamma(\alpha)} \int_0^t (t-s)^{\alpha-1} \left(d_1 u_{xx} + a_1 - (b_1 + w(x, s))u(x, s) + u^2(x, s)v(x, s) \right. \\ &\quad \left. + f_1(x, s) \right) ds, \end{aligned} \quad (4.28)$$

$$\begin{aligned} v(x, t) - v(x, 0) &= \frac{1}{\Gamma(\alpha)} \int_0^t (t-s)^{\alpha-1} \left(d_2 v_{xx} + u(x, s)w(x, s) - u^2(x, s)v(x, s) \right. \\ &\quad \left. + f_2(x, s) \right) ds, \end{aligned} \quad (4.29)$$

and

$$w(x, t) - w(x, 0) = \frac{1}{\Gamma(\alpha)} \int_0^t (t-s)^{\alpha-1} \left(d_3 w_{xx} - u(x, s)w(x, s) + c_1 + f_3(x, s) \right) ds. \quad (4.30)$$

Let

$$K_1(t, u(x, t)) = d_1 u_{xx} + a_1 - (b_1 + w)u + u^2 v + f_1(x, t), \quad (4.31)$$

$$K_2(t, v(x, t)) = d_2 v_{xx} + uw - u^2 v + f_2(x, t), \quad (4.32)$$

and

$$K_3(t, w(x, t)) = d_3 w_{xx} - uw + c_1 + f_3(x, t), \quad (4.33)$$

and for continuous function $u(x, t)$, $u_1(x, t)$, $v(x, t)$, $v_1(x, t)$, $w(x, t)$ and $w_1(x, t) \in L^2((0, 1) \times (0, 1))$, there exist some constant $\gamma_1 > 0$, $\gamma_2 > 0$ and $\gamma_3 > 0$ such that

$$\begin{aligned} \|u_{xx} - (u_1)_{xx}\| &\leq \gamma_1 \|u - u_1\|, \\ \|v_{xx} - (v_1)_{xx}\| &\leq \gamma_2 \|v - v_1\|, \\ \|w_{xx} - (w_1)_{xx}\| &\leq \gamma_3 \|w - w_1\|. \end{aligned} \quad (4.34)$$

Also, here $|d_1| \leq s_1$, $|b_1| \leq s_2$, $|d_2| \leq l_1$, $|d_3| \leq l_2$ and, now, we will show that $K_1(t, u(x, t))$, $K_2(t, v(x, t))$ and $K_3(t, w(x, t))$ satisfy the Lipschitz condition, for this purpose, we have

$$\begin{aligned} \|K_1(t, u) - K_1(t, u_1)\| &= \|d_1 u_{xx} + a_1 - (b_1 + w)u + u^2 v + f_1(x, t) - (d_1 (u_1)_{xx} \\ &\quad + a_1 - (b_1 + w)u_1 + u_1^2 v + f_1(x, t))\|, \\ &\leq |d_1| \gamma_1 \|u - (u_1)\| + (|b_1| + |w|) \|u - u_1\| + |v| \|u^2 - u_1^2\|, \\ &\leq \left(s_1 \gamma_1 + (s_2 + s_3) + s_4 (\lambda_1 + \lambda_2) \right) \|u - u_1\|. \end{aligned} \quad (4.35)$$

Setting,

$$M_1 = s_1 \gamma_1 + (s_2 + s_3) + s_4 (\lambda_1 + \lambda_2),$$

where u and u_1 are bounded function such that $|u| \leq \lambda_1$ and $|u_1| \leq \lambda_2$ then, we have

$$\|K_1(t, u) - K_1(t, u_1)\| \leq M_1 \|u - u_1\|. \quad (4.36)$$

Similarly, for the functions $v(x, t)$ and $w(x, t)$, we have

$$\|K_2(t, v) - K_2(t, v_1)\| \leq M_2 \|v - v_1\|, \quad (4.37)$$

$$\|K_3(t, w) - K_3(t, w_1)\| \leq M_3 \|w - w_1\|, \quad (4.38)$$

where $M_2 = (l_1\gamma_2 + \lambda_1^2)$ and $M_3 = (l_2\gamma_3 + \lambda_1)$. Hence Lipschitz condition is satisfied by the kernel $K_1(t, u)$, $K_2(t, v)$ and $K_3(t, w)$. In addition if $0 \leq M_i < 1$, $i = 1, 2, 3$, then it is contraction.

Theorem 4.5. *Let us assume that $u(x, t)$, $v(x, t)$ and $w(x, t)$ are bounded functions, then the operators $\Phi(u(x, t))$, $\Phi(v(x, t))$ and $\Phi(w(x, t))$ defined by [118]*

$$\Phi(u(x, t)) = u(x, 0) + \frac{1}{\Gamma(\alpha)} \int_0^t (t-s)^{\alpha-1} K_1(x, u) ds, \quad (4.39)$$

$$\Phi(v(x, t)) = v(x, 0) + \frac{1}{\Gamma(\alpha)} \int_0^t (t-s)^{\alpha-1} K_2(x, v) ds, \quad (4.40)$$

and

$$\Phi(w(x, t)) = w(x, 0) + \frac{1}{\Gamma(\alpha)} \int_0^t (t-s)^{\alpha-1} K_3(x, w) ds, \quad (4.41)$$

satisfy the Lipschitz condition.

Proof. Assume that $u(x, t)$ and $u_1(x, t)$ are bounded function such that $u(x, 0) = u_1(x, 0)$, then

$$\begin{aligned} \Phi(u(x, t)) - \Phi(u_1(x, t)) &= \frac{1}{\Gamma(\alpha)} \int_0^t (t-s)^{\alpha-1} (K_1(x, u) - K_1(x, u_1)) ds, \\ \|\Phi(u(x, t)) - \Phi(u_1(x, t))\| &\leq \frac{1}{\Gamma(\alpha)} \int_0^t (t-s)^{\alpha-1} \|K_1(x, u) - K_1(x, u_1)\| ds, \\ &\leq \frac{\gamma_0^\alpha M_1}{\Gamma(1+\alpha)} \|u - u_1\|. \end{aligned}$$

Considering $m_1 = \frac{\gamma_0^\alpha M_1}{\Gamma(\alpha+1)}$, we get

$$\|\Phi(u(x, t)) - \Phi(u_1(x, t))\| \leq m_1 \|u - u_1\|.$$

Similarly, by assuming $v(x, t)$, $v_1(x, t)$, $w(x, t)$ and $w_1(x, t)$ as bounded functions we can show that

$$\|\Phi(v(x, t)) - \Phi(v_1(x, t))\| \leq m_2 \|v - v_1\|,$$

$$\|\Phi(w(x, t)) - \Phi(w_1(x, t))\| \leq m_3 \|w - w_1\|.$$

Hence the proof is completed. \square

Theorem 4.6. *Let us assume that $u(x, t)$, $v(x, t)$ and $w(x, t)$ are bounded functions, then the operators defined by*

$$\Phi(u) = d_1 u_{xx} + a_1 - (b_1 + w)u + u^2 v + f_1(x, t), \quad (4.42)$$

$$\Phi(v) = d_2 v_{xx} + uw - u^2 v + f_2(x, t), \quad (4.43)$$

and

$$\Phi(w) = d_3 w_{xx} - uw + c_1 + f_3(x, t), \quad (4.44)$$

satisfy the conditions

$$\left| \left\langle \Phi(u) - \Phi(u_1), u - u_1 \right\rangle \right| \leq M_1 \|u - u_1\|^2, \quad (4.45)$$

$$\left| \left\langle \Phi(v) - \Phi(v_1), v - v_1 \right\rangle \right| \leq M_2 \|v - v_1\|^2, \quad (4.46)$$

and

$$\left| \left\langle \Phi(w) - \Phi(w_1), w - w_1 \right\rangle \right| \leq M_3 \|w - w_1\|^2, \quad (4.47)$$

respectively.

Proof. By considering the function $u(x, t)$ as bounded function, we have

$$\begin{aligned} \left| \left\langle \Phi(u) - \Phi(u_1), u - u_1 \right\rangle \right| &= \left| \left\langle d_1(u_{xx} - (u_1)_{xx}) - b_1(u - u_1) - w(u - u_1) + v(u^2 - u_1^2), u - u_1 \right\rangle \right|, \\ &\leq |d_1| | \langle (u - u_1)_{xx}, u - u_1 \rangle | + |b_1| | \langle u - u_1, u - u_1 \rangle | + |w| \\ &| \langle u - u_1, u - u_1 \rangle | + |v| | \langle u^2 - u_1^2, u - u_1 \rangle |, \\ &\leq |d_1| | \langle (u - u_1)_{xx}, u - u_1 \rangle | |u - u_1| + |b_1| |u - u_1|^2 + |w| |u - u_1|^2 \\ &+ |v| |u - u_1|^2 |u + u_1|, \end{aligned}$$

i.e.,

$$\left| \left\langle \Phi(u) - \Phi(u_1), u - u_1 \right\rangle \right| \leq \left(s_1 \gamma_1 + (s_2 + s_3) + s_4 (\lambda_1 + \lambda_2) \right) \|u - u_1\|^2,$$

which implies that

$$\left| \left\langle \Phi(u) - \Phi(u_1), u - u_1 \right\rangle \right| \leq M_1 \|u - u_1\|^2.$$

Repeating this same process for the bounded functions $v(x, t)$ and $w(x, t)$, we have

$$\left| \left\langle \Phi(v) - \Phi(v_1), v - v_1 \right\rangle \right| \leq M_2 \|v - v_1\|^2,$$

and

$$\left| \left\langle \Phi(w) - \Phi(w_1), w - w_1 \right\rangle \right| \leq M_3 \|w - w_1\|^2.$$

□

Theorem 4.7. Suppose that $u(x, t)$, $v(x, t)$ and $w(x, t)$ are bounded functions and $0 < \|z\| < \infty$, then the operators

$$\Phi(u) = d_1 u_{xx} + a_1 - (b_1 + w)u + u^2 v + f_1(x, t), \quad (4.48)$$

$$\Phi(v) = d_2 v_{xx} + uv - u^2 v + f_2(x, t), \quad (4.49)$$

and

$$\phi(w) = d_3 w_{xx} - uw + c_1 + f_3(x, t), \quad (4.50)$$

satisfy the conditions

$$\left| \langle \Phi(u) - \Phi(u_1), z \rangle \right| \leq M_1 \|u - u_1\| \|z\|, \quad (4.51)$$

$$\left| \langle \Phi(v) - \Phi(v_1), z \rangle \right| \leq M_2 \|v - v_1\| \|z\|, \quad (4.52)$$

and

$$\left| \langle \Phi(w) - \Phi(w_1), z \rangle \right| \leq M_3 \|w - w_1\| \|z\|, \quad (4.53)$$

respectively.

Proof. Let $u(x, t)$ is bounded function and $0 < \|z\| < \infty$, then we have

$$\begin{aligned} \left| \langle \Phi(u) - \Phi(u_1), z \rangle \right| &= \left| \langle d_1(u_{xx} - (u_1)_{xx}) - b_1(u - u_1) - w(u - u_1) + v(u^2 - u_1^2), z \rangle \right| \\ &\leq |d_1| |\langle (u - u_1)_{xx}, z \rangle| + |b_1| |\langle u - u_1, z \rangle| + |w| |\langle u - u_1, z \rangle| \\ &\quad + |v| |\langle u^2 - u_1^2, z \rangle|, \\ &\leq |d_1| \|(u - u_1)_{xx}\| \|z\| + |b_1| \|u - u_1\| \|z\| + |w| \|u - u_1\| \|z\| \\ &\quad + |v| \|u - u_1\| \|z\|, \end{aligned}$$

$$\left| \langle \Phi(u) - \Phi(u_1), z \rangle \right| \leq (s_1 \gamma_1 + (s_2 + s_3) + s_4(\lambda_1 + \lambda_2)) \|u - u_1\| \|z\|,$$

which implies that

$$\left| \langle \Phi(u) - \Phi(u_1), z \rangle \right| \leq M_1 \|u - u_1\| \|z\|.$$

Repeating this same process for the bounded functions $v(x, t)$ and $w(x, t)$, we have

$$\left| \left\langle \Phi(v) - \Phi(v_1), z \right\rangle \right| \leq M_2 \|v - v_1\| \|z\|,$$

$$\left| \left\langle \Phi(w) - \Phi(w_1), z \right\rangle \right| \leq M_3 \|w - w_1\| \|z\|.$$

Hence proof is complete. □

Now, the iterated formula for Eqs.(4.28) – (4.30) are formulated as

$$u_{n+1}(x, t) = \frac{1}{\Gamma(\alpha)} \int_0^t (t-s)^{\alpha-1} K_1(t, u_n) ds, \quad (4.54)$$

$$v_{n+1}(x, t) = \frac{1}{\Gamma(\alpha)} \int_0^t (t-s)^{\alpha-1} K_2(t, v_n) ds, \quad (4.55)$$

$$w_{n+1}(x, t) = \frac{1}{\Gamma(\alpha)} \int_0^t (t-s)^{\alpha-1} K_3(t, w_n) ds, \quad (4.56)$$

with $u(x, 0) = u_0$, $v(x, 0) = v_0$ and $w(x, 0) = w_0$.

The successive difference is presented in the following way

$$\begin{aligned} \xi_n(x, t) = u_n(x, t) - u_{n-1}(x, t) &= \frac{1}{\Gamma(\alpha)} \int_0^t (t-s)^{\alpha-1} \left(K_1(t, u_{n-1}) \right. \\ &\quad \left. - K_1(t, u_{n-2}) \right) ds, \end{aligned} \quad (4.57)$$

$$\begin{aligned} \chi_n(x, t) = v_n(x, t) - v_{n-1}(x, t) &= \frac{1}{\Gamma(\alpha)} \int_0^t (t-s)^{\alpha-1} \left(K_2(t, v_{n-1}) \right. \\ &\quad \left. - K_2(t, v_{n-2}) \right) ds, \end{aligned} \quad (4.58)$$

and

$$\eta_n(x, t) = w_n(x, t) - w_{n-1}(x, t) = \frac{1}{\Gamma(\alpha)} \int_0^t (t-s)^{\alpha-1} \left(K_3(t, w_{n-1}) - K_3(t, w_{n-2}) \right) ds. \quad (4.59)$$

Note that

$$u_n(x, t) = \sum_{i=0}^n \xi_i(x, t), \quad (4.60)$$

$$v_n(x, t) = \sum_{j=0}^n \chi_j(x, t), \quad (4.61)$$

$$w_n(x, t) = \sum_{k=0}^n \eta_k(x, t), \quad (4.62)$$

Applying norm on both sides of the Eq.(4.57), we get

$$\|\xi_n(x, t)\| = \left\| \frac{1}{\Gamma(\alpha)} \int_0^t (t-s)^{\alpha-1} \left(K_1(t, u_{n-1}) - K_1(t, u_{n-2}) \right) ds \right\|, \quad (4.63)$$

or

$$\|\xi_n(x, t)\| \leq \frac{1}{\Gamma(\alpha)} \int_0^t (t-s)^{\alpha-1} \left\| \left(K_1(t, u_{n-1}) - K_1(t, u_{n-2}) \right) \right\| ds. \quad (4.64)$$

As Lipschitz condition is satisfied by the kernel, thus

$$\|\xi_n(x, t)\| \leq \frac{M_1}{\Gamma(\alpha)} \int_0^t (t-s)^{\alpha-1} \|u_{n-1} - u_{n-2}\| ds. \quad (4.65)$$

Proceeding in same process for the bounded functions $v(x, t)$ and $w(x, t)$, we get

$$\|\chi_n(x, t)\| \leq \frac{M_2}{\Gamma(\alpha)} \int_0^t (t-s)^{\alpha-1} \|v_{n-1} - v_{n-2}\| ds, \quad (4.66)$$

and

$$\|\eta_n(x, t)\| \leq \frac{M_3}{\Gamma(\alpha)} \int_0^t (t-s)^{\alpha-1} \|w_{n-1} - w_{n-2}\| ds. \quad (4.67)$$

Based on the above results, we can prove the following theorem.

Theorem 4.8. *Three-component Brusselator reaction-diffusion system defined in Eq.(4.1) has a solution if there exists γ_0 such that*

$$\frac{M_i \gamma_0^\alpha}{\Gamma(\alpha + 1)} < 1, \quad i = 1, 2, 3. \quad (4.68)$$

Proof. Considering $u(x, t)$ as bounded function and performing the recursive scheme, we have

$$\|\xi_n(x, t)\| \leq \left[\frac{M_1 t^\alpha}{\Gamma(\alpha + 1)} \right]^n u(x, 0), \quad (4.69)$$

and thus the function

$$u_n(x, t) = \sum_{i=0}^n \xi_i(x, t),$$

exists and smooth. Now, to show that Eq.(4.60) is a solution of Eq.(4.1), let us assume that $u(x, t) - u(x, 0) = u_n(x, t) - L_n(x, t)$, then we have

$$\begin{aligned} \|L_n(x, t)\| &= \left\| \frac{1}{\Gamma(\alpha)} \int_0^t (t-s)^{\alpha-1} \left(K_1(t, u) - K_1(t, u_{n-1}) \right) ds \right\|, \\ &\leq \left[\frac{M_1 t^\alpha}{\Gamma(\alpha + 1)} \right] \|u - u_{n-1}\|. \end{aligned} \quad (4.70)$$

Recursively, we get

$$\|L_n(x, t)\| \leq \left[\frac{t^\alpha}{\Gamma(\alpha + 1)} \right]^{n+1} M_1^{n+1} \epsilon_1. \quad (4.71)$$

At $t = \gamma_0$, the above equation becomes

$$\|L_n(x, t)\| \leq \left[\frac{\gamma_0^\alpha}{\Gamma(\alpha + 1)} \right]^{n+1} M_1^{n+1} \epsilon_1. \quad (4.72)$$

If $n \rightarrow \infty$, then $\|L_n(x, t)\| \rightarrow 0$.

Similarly for the functions $v(x, t)$ and $w(x, t)$, we have

$$\|d_n(x, t)\| \leq \left[\frac{\gamma_0^\alpha}{\Gamma(\alpha + 1)} \right]^{n+1} M_2^{n+1} \epsilon_2, \quad (4.73)$$

and

$$\|S_n(x, t)\| \leq \left[\frac{\gamma_0^\alpha}{\Gamma(\alpha + 1)} \right]^{n+1} M_3^{n+1} \epsilon_3, \quad (4.74)$$

which tend to zero as $n \rightarrow \infty$

Hence the proof is completed. \square

Let us proceed, next, to examine whether or not there is any unique solution to the fractional order Brusselator reaction-diffusion system (4.1). Let $u(x, t)$ and $r(x, t)$ are two solutions of the system (4.1), then we have

$$u(x, t) - r(x, t) = \frac{1}{\Gamma(\alpha)} \int_0^t (t-s)^{\alpha-1} (K_1(t, u) - K_1(t, r)) ds. \quad (4.75)$$

If we take the norm on both sides of Eq.(4.75), we get

$$\|u(x, t) - r(x, t)\| = \left\| \frac{1}{\Gamma(\alpha)} \int_0^t (t-s)^{\alpha-1} (K_1(t, u) - K_1(t, r)) ds \right\|, \quad (4.76)$$

or

$$\|u(x, t) - r(x, t)\| \leq \left(\frac{M_1 t^\alpha}{\Gamma(\alpha + 1)} \right) \|u(x, t) - r(x, t)\|, \quad (4.77)$$

which implies that

$$\|u(x, t) - r(x, t)\| \left(1 - \frac{M_1 \gamma^\alpha}{\Gamma(\alpha + 1)} \right) \leq 0, \quad (4.78)$$

where γ is a positive constant.

Similarly, for the functions $v(x, t)$ and $w(x, t)$, we get

$$\|v(x, t) - r_1(x, t)\| \left(1 - \frac{M_2 \gamma^\alpha}{\Gamma(\alpha + 1)}\right) \leq 0, \quad (4.79)$$

$$\|w(x, t) - r_2(x, t)\| \left(1 - \frac{M_3 \gamma^\alpha}{\Gamma(\alpha + 1)}\right) \leq 0. \quad (4.80)$$

Theorem 4.9. *A fractional Brusselator reaction-diffusion system has a unique solution if the following conditions are met.*

$$\left(1 - \frac{M_i \gamma^\alpha}{\Gamma(\alpha + 1)}\right) > 0, \quad i = 1, 2, 3. \quad (4.81)$$

Proof. We have the following result if the condition of the previous Theorem is satisfied

$$\|u(x, t) - r(x, t)\| \left(1 - \frac{M_1 \gamma^\alpha}{\Gamma(\alpha + 1)}\right) \leq 0. \quad (4.82)$$

Consequently, it implies that

$$\|u(x, t) - r(x, t)\| = 0,$$

as a result $u(x, t) = r(x, t)$.

Similarly, we can show it for $v(x, t)$ and $w(x, t)$.

Hence the system (4.1) has a unique solution. \square

4.4.2 Ulam-Hyers stability

Our goal is to demonstrate that the VOFFN system presented in Eq.(4.1) is Ulam-Hyers stable.

Definition This Eq.(4.1) is Ulam-Hyers stable if the following relations hold for $\delta_1, \delta_2, \delta_3 > 0$ [119].

$$|{}_0^c D_t^\alpha u - d_1 u_{xx} - a_1 + (b_1 + w)u - u^2 v - f_1(x, t)| < \delta_1, \quad (4.83)$$

$$|{}_0^c D_t^\alpha v - d_2 v_{xx} - uw + u^2 v - f_2(x, t)| < \delta_2, \quad (4.84)$$

and

$$|{}_0^c D_t^\alpha w - d_3 w_{xx} + uw - c_1 - f_3(x, t)| < \delta_3. \quad (4.85)$$

Then there exist solutions u^*, v^* and w^* , such that

$$|u - u^*| < a'_1 \delta_1, \quad |v - v^*| < a'_2 \delta_2, \quad a'_1, a'_2 \in \mathbb{R}, \quad (4.86)$$

and

$$|w - w^*| < a'_3 \delta_3, \quad a'_3 \in \mathbb{R}. \quad (4.87)$$

When u, v and w satisfy Eqs.(4.83)–(4.84) and Eq.(4.85), then there exists functions $q_1(x, t), q_2(x, t)$ and $q_3(x, t)$ which are defined as follows:

$${}_0^c D_t^\alpha u - d_1 u_{xx} - a_1 + (b_1 + w)u - u^2 v - f_1(x, t) = q_1(x, t), \quad (4.88)$$

$${}_0^c D_t^\alpha v - d_2 v_{xx} - uw + u^2 v - f_2(x, t) = q_2(x, t), \quad (4.89)$$

and

$${}_0^c D_t^\alpha w - d_3 w_{xx} + uw - c_1 - f_3(x, t) = q_3(x, t). \quad (4.90)$$

Using RL fractional integral to both sides of Eq.(4.88), we achieve

$$u(x, t) - u(x, 0) + I_t^\alpha \left(-d_1 u_{xx} - a_1 + (b_1 + w)u - u^2 v - f_1(x, t) \right) = I_t^\alpha q_1(x, t). \quad (4.91)$$

Now,

$$\begin{aligned} |u(x, t) - u(x, 0) + I_t^\alpha(-d_1 u_{xx} - a_1 + (b_1 + w)u - u^2 v - f_1(x, t))| &= |I_t^\alpha q_1(x, t)| \\ &\leq |q_1| |I_t^\alpha(1)| = |q_1| \frac{T^\alpha}{\Gamma(\alpha + 1)}, \end{aligned}$$

$$|u(x, t) - u(x, 0) + I_t^\alpha(-d_1 u_{xx} - a_1 + (b_1 + w)u - u^2 v - f_1(x, t))| \leq \frac{T^\alpha}{\Gamma(\alpha + 1)} \delta_1.$$

Similarly for $v(x, t)$ and $w(x, t)$,

$$|v(x, t) - v(x, 0) + I_t^\alpha(-d_2 v_{xx} - uw + u^2 v - f_2)| \leq \frac{T^\alpha}{\Gamma(\alpha + 1)} \delta_2,$$

$$|w(x, t) - w(x, 0) + I_t^\alpha(-d_3 w_{xx} + uw - c_1 - f_3(x, t))| \leq \frac{T^\alpha}{\Gamma(\alpha + 1)} \delta_3.$$

Suppose that $u^*(x, t)$, $v^*(x, t)$ and $w^*(x, t)$ be the solutions of system (4.1) with $u(x, 0) = u^*(x, 0) = g_0$, $v(x, 0) = v^*(x, 0) = g_1$, and $w(x, 0) = w^*(x, 0) = g_2$, then

$$u^*(x, t) = u(x, 0) + I_t^\alpha \left(d_1 u_{xx} + a_1 - (b_1 + w)u + u^2 v + f_1(x, t) \right).$$

Therefore,

$$\|u - u^*\| = \|u - u(x, 0) - I_t^\alpha(d_1 u_{xx} + a_1 - (b_1 + w)u + u^2 v + f_1(x, t))\|,$$

$$\begin{aligned} \|u - u^*\| &= \|u - u(x, 0) - I_t^\alpha(d_1 u_{xx}(x, t) + a_1 - (b_1 + w(x, t))u(x, t) + \\ &\quad u^2(x, t)v(x, t) + f_1(x, t)) - I_t^\alpha(d_1 u_{xx}^*(x, t) + a_1 - (b_1 + w(x, t))u^*(x, t) + \\ &\quad (u^*)^2(x, t)v(x, t) + f_1(x, t)) + I_t^\alpha(d_1 u_{xx}^*(x, t) + a_1 - (b_1 + w(x, t)) \times \\ &\quad u^*(x, t) + (u^*)^2(x, t)v(x, t) + f_1(x, t))\|, \end{aligned}$$

i.e.,

$$\|u - u^*\| \leq \frac{T^\alpha}{\Gamma(\alpha + 1)} \delta_1 + \left(s_1 \gamma_1 + (s_2 + s_3) + s_4(\lambda_1 + \lambda_2) \right) (I_t^\alpha (\|u - u^*\|)). \quad (4.92)$$

Similarly for the functions $v(x, t)$ and $w(x, t)$, we obtain

$$\|v - v^*\| \leq \frac{T^\alpha}{\Gamma(\alpha + 1)} \delta_2 + (l_1 \gamma_2 + \lambda_1^2) (I_t^\alpha \|v - v^*\|), \quad (4.93)$$

$$\|w - w^*\| \leq \frac{T^\alpha}{\Gamma(\alpha + 1)} \delta_3 + (l_2 \gamma_3 + \lambda_1) (I_t^\alpha \|w - w^*\|). \quad (4.94)$$

Lemma: Let $\alpha > 0$ and $z_1(x, t)$ be locally integrable, non-negative and non-decreasing function on interval (a, b) . Also, let $u(x, t)$ be non-negative and locally integrable on interval $[a, b)$ and $z_2(x, t)$ is bounded by some constant, then the inequality given by [120]

$$u(x, t) \leq z_1(x, t) + z_2(x, t) \left(I_t^\alpha u(x, t) \right), \quad (4.95)$$

implies

$$u(x, t) \leq z_1(x, t) \mathbf{E}_\alpha \left(z_2(x, t) (t - a)^t \right), \quad (4.96)$$

where $\mathbf{E}_\alpha(t) = \sum_{r=0}^{\infty} \frac{t^r}{\Gamma(\alpha r + 1)}$.

We obtain the following result by applying the Gronwall relation to Eq.(4.92) with

$$z_1(x, t) = \frac{T^\alpha}{\Gamma(\alpha + 1)} \delta_1 \text{ and } z_2(x, t) = \left(s_1 \gamma_1 + (s_2 + s_3) + s_4(\lambda_1 + \lambda_2) \right).$$

$$\begin{aligned} \|u - u^*\| &\leq \frac{T^\alpha}{\Gamma(\alpha + 1)} \delta_1 \mathbf{E}_\alpha \left(\left(s_1 \gamma_1 + (s_2 + s_3) + s_4(\lambda_1 + \lambda_2) \right) t^\alpha \right), \\ &\leq \frac{T^\alpha}{\Gamma(\alpha + 1)} \delta_1 \mathbf{E}_\alpha \left(\left(s_1 \gamma_1 + (s_2 + s_3) + s_4(\lambda_1 + \lambda_2) \right) T^\alpha \right). \end{aligned} \quad (4.97)$$

Applying the Gronwall relation to Eq.(4.93) and Eq.(4.94), we get

$$\|v - v^*\| \leq \frac{T^\alpha}{\Gamma(\alpha + 1)} \delta_2 \mathbf{E}_\alpha \left((l_1 \gamma_2 + \lambda_1^2) T^\alpha \right), \quad (4.98)$$

$$\|w - w^*\| \leq \frac{T^\alpha}{\Gamma(\alpha + 1)} \delta_3 \mathbf{E}_\alpha \left((l_2 \gamma_3 + \lambda_1) T^\alpha \right). \quad (4.99)$$

Eqs.(4.97)-(4.99), imply $\|u - u^*\| \leq a'_1 \delta_1$, $\|v - v^*\| \leq a'_1 \delta_2$ and $\|w - w^*\| \leq a'_1 \delta_3$, with

$$a'_1 = \frac{T^\alpha}{\Gamma(\alpha + 1)} \delta_1 \mathbf{E}_\alpha \left(\left(s_1 \gamma_1 + (s_2 + s_3) + s_4 (\lambda_1 + \lambda_2) \right) T^\alpha \right),$$

and

$$a'_2 = \frac{T^\alpha}{\Gamma(\alpha + 1)} \delta_2 \mathbf{E}_\alpha \left((l_1 \gamma_2 + \lambda_1^2) T^\alpha \right), \quad a'_3 = \frac{T^\alpha}{\Gamma(\alpha + 1)} \delta_3 \mathbf{E}_\alpha \left((l_2 \gamma_3 + \lambda_1) T^\alpha \right).$$

The solution of Eq.(4.1) is therefore Ulam-Hyers stable.

4.5 Implementation of the approach

In this section a detailed, step-by-step implementation of the combined wavelet operational matrix and collocation method for solving FPDE have been provided.

Consider the model (4.1) under the following ICs and BCs:

$$\begin{aligned} u(x, 0) &= u_0(x), & v(x, 0) &= v_0(x), & w(x, 0) &= w_0(x), \\ u(0, t) &= u_1(t), & v(0, t) &= v_1(t), & w(0, t) &= w_1(t), \\ u(1, t) &= u_2(t), & v(1, t) &= v_2(t), & w(1, t) &= w_2(t). \end{aligned} \quad (4.100)$$

Let us assume the following approximation for $u(x, t)$, $v(x, t)$ and $w(x, t)$ as

$$\begin{aligned}
u(x, t) &\simeq \sum_{i=1}^{\hat{m}} \sum_{j=1}^{\hat{m}} u_{ij} \psi_i(x) \psi_j(t), \\
&\triangleq \Psi^T(x) \mathbf{U} \Psi(t), \\
v(x, t) &\simeq \sum_{i=1}^{\hat{m}} \sum_{j=1}^{\hat{m}} v_{ij} \psi_i(x) \psi_j(t), \\
&\triangleq \Psi^T(x) \mathbf{V} \Psi(t), \\
w(x, t) &\simeq \sum_{i=1}^{\hat{m}} \sum_{j=1}^{\hat{m}} w_{ij} \psi_i(x) \psi_j(t), \\
&\triangleq \Psi^T(x) \mathbf{W} \Psi(t),
\end{aligned} \tag{4.101}$$

where \mathbf{U} , \mathbf{V} and \mathbf{W} are unknown matrices of order $\hat{m} \times \hat{m}$ to be determined and $\Psi(x)$ is vector defined in Eq.(4.12). Theorem 4.2 yield

$$\begin{aligned}
\frac{\partial^2 u(x, t)}{\partial x^2} &\simeq \Psi^T(x) (D^{(2)})^T \mathbf{U} \Psi(t), \\
\frac{\partial^2 v(x, t)}{\partial x^2} &\simeq \Psi^T(x) (D^{(2)})^T \mathbf{V} \Psi(t), \\
\frac{\partial^2 w(x, t)}{\partial x^2} &\simeq \Psi^T(x) (D^{(2)})^T \mathbf{W} \Psi(t).
\end{aligned} \tag{4.102}$$

Also, from Theorem 4.4, we get

$$\begin{aligned}
\frac{\partial^\alpha u(x, t)}{\partial t^\alpha} &\simeq \Psi^T(x) \mathbf{U} (B^\alpha) \Psi(t), \\
\frac{\partial^\alpha v(x, t)}{\partial t^\alpha} &\simeq \Psi^T(x) \mathbf{V} (B^\alpha) \Psi(t), \\
\frac{\partial^\alpha w(x, t)}{\partial t^\alpha} &\simeq \Psi^T(x) \mathbf{W} (B^\alpha) \Psi(t).
\end{aligned} \tag{4.103}$$

The residual function can be obtained by inserting Eqs.(4.101)-(4.103) into the Eq.(4.1) as

$$R_1(x, t) \triangleq -\Psi^T(x)\mathbf{U}\left(B^\alpha\right)\Psi(t) + d_1 \Psi^T(x)(D^{(2)})^T\mathbf{U}\Psi(t) + a_1 - (b_1 + \Psi^T(x)\mathbf{W}\Psi(t)) \\ \times (\Psi^T(x)\mathbf{U}\Psi(t)) + \left(\Psi^T(x)\mathbf{U}\Psi(t)\right)^2 + \left(\Psi^T(x)\mathbf{V}\Psi(t)\right) + f_1(x, t), \quad (4.104)$$

$$R_2(x, t) \triangleq -\Psi^T(x)\mathbf{V}\left(B^\alpha\right)\Psi(t) + d_2 (D^2\Psi(x))^T\mathbf{V}\Psi(t) + \Psi^T(x)\mathbf{U}\Psi(t)\Psi^T(x)\mathbf{W}\Psi(t) \\ - (\Psi^T(x)\mathbf{U}\Psi(t))^2(\Psi^T(x)\mathbf{V}\Psi(t)) + f_2(x, t), \quad (4.105)$$

$$R_3(x, t) \triangleq -\Psi^T(x)\mathbf{W}\left(B^\alpha\right)\Psi(t) + d_3 (D^2\Psi(x))^T\mathbf{W}\Psi(t) - (\Psi^T(x)\mathbf{U}\Psi(t)) \\ \times (\Psi^T(x)\mathbf{W}\Psi(t)) + c_1 + f_3(x, t). \quad (4.106)$$

Now, associated initial and boundary conditions can be approximated via VF wavelets as

$$\Psi(x)^T\mathbf{U}\Psi(0) - u_0(x) \triangleq U_0(x) \simeq 0, \quad \Psi(x)^T\mathbf{V}\Psi(0) - v_0(x) \triangleq V_0(x) \simeq 0, \quad (4.107)$$

$$\Psi(x)^T\mathbf{W}\Psi(0) - w_0(x) \triangleq W_0(x) \simeq 0, \quad (4.108)$$

and

$$\Psi(0)^T\mathbf{U}\Psi(t) - u_1(t) \triangleq U_1(t) \simeq 0, \quad \Psi(1)^T\mathbf{U}\Psi(t) - u_2(t) \triangleq U_2(t) \simeq 0, \\ \Psi(0)^T\mathbf{V}\Psi(t) - v_1(t) \triangleq V_1(t) \simeq 0, \quad \Psi(1)^T\mathbf{V}\Psi(t) - v_2(t) \triangleq V_2(t) \simeq 0, \quad (4.109) \\ \Psi(0)^T\mathbf{W}\Psi(t) - w_1(t) \triangleq W_1(t) \simeq 0, \quad \Psi(1)^T\mathbf{W}\Psi(t) - w_2(t) \triangleq W_2(t) \simeq 0.$$

At this stage collocating Eqs.(4.104)-(4.109) at the certain collocation points i.e.,

$$\left\{ \begin{array}{l} R_r(x_i, t_j) = 0, \quad r = 1, 2, 3 \quad 2 \leq i \leq \hat{m} - 1, \quad 2 \leq j \leq \hat{m}, \\ U_0(x_i) = 0, \quad V_0(x_i) = 0, \quad W_0(x_i) = 0, \quad 1 \leq i \leq \hat{m}, \\ U_1(t_j) = 0, \quad U_2(t_j) = 0, \quad 2 \leq j \leq \hat{m}, \\ V_1(t_j) = 0, \quad V_2(t_j) = 0, \quad 2 \leq j \leq \hat{m}, \\ W_1(t_j) = 0, \quad W_2(t_j) = 0, \quad 2 \leq j \leq \hat{m}. \end{array} \right. \quad (4.110)$$

This system (4.110) generates $3(\hat{m} \times \hat{m})$ equations. To derive a numerical solution to the original system, one has to solve these algebraic equations for computing the unknown matrices.

4.6 Error bound analysis

Theorem 4.10. *Suppose that $f(x, y)$ is a function of two variables which is continuous and defined in $[0, 1] \times [0, 1]$ having the property $\left| \frac{\partial^4 f(x, y)}{\partial x^2 \partial y^2} \right| < B$, then for any positive integer k ,*

(i) *the series expansion of $f(x, y)$ as*

$$f(x, y) = \sum_{n=0}^{2^k-1} \sum_{n'=0}^{2^k-1} \sum_{m=1}^M \sum_{m'=1}^M c_{n, n', m, m'} \psi_{n, m}(x) \psi_{n', m'}(y),$$

converges uniformly to $f(x, y)$.

(ii)

$$\sigma_{f, k, M}^2 < \frac{9\pi}{32} \sum_{n=2^k}^{\infty} \sum_{m=1+M}^{\infty} \sum_{n'=2^k}^{\infty} \sum_{m'=1+M}^{\infty} \frac{B}{(n+1)^2(m-2)^4(n'+1)^2(m'-2)^4}.$$

Proof. (i)

$$\begin{aligned} c_{n,m,n',m'} &= \int_0^1 \int_0^1 f(x,y) \psi_{n,m}(x) \omega_n(x) \psi_{n',m'}(y) \omega'_n(y) dx dy, \\ &= \int_{\frac{n}{2^k}}^{\frac{n+1}{2^k}} \int_{\frac{n'}{2^k}}^{\frac{n'+1}{2^k}} f(x,y) 2^{2k} \sqrt{\frac{8}{\pi}} \times \sqrt{\frac{8}{\pi}} VF_m^*(2^k x - n) w(2^k x - n) VF_{m'}^*(2^k y - n') \\ &\quad \times w(2^k y - n') dx dy. \end{aligned}$$

Now, let $2^k x - n = \gamma$ and $2^k y - n' = \gamma_1$. Therefore

$$c_{n,m,n',m'} = \sqrt{\frac{8}{\pi}} \times \sqrt{\frac{8}{\pi}} \int_0^1 \int_0^1 f\left(\frac{\gamma+n}{2^k}, \frac{\gamma_1+n'}{2^k}\right) VF^*(\gamma) w(\gamma) VF^*(\gamma_1) w(\gamma_1) d\gamma d\gamma_1.$$

Substituting $\gamma = \frac{2+2\cos(\omega_1)}{4}$ and $\gamma_1 = \frac{2+2\cos(\omega_2)}{4}$ in the above equation, we have

$$\begin{aligned} c_{n,m,n',m'} &= \sqrt{\frac{1}{2\pi}} \times \sqrt{\frac{1}{2\pi}} \int_0^\pi \int_0^\pi f\left(\frac{2n+\cos\omega_1+1}{2^{k+1}}, \frac{2n'+\cos\omega_2+1}{2^{k+1}}\right) \sin m\omega_1 \sin \omega_1 \\ &\quad \times \sin m'\omega_2 \sin \omega_2 d\omega_1 d\omega_2, \\ &= \left(\frac{1}{8}\sqrt{\frac{8}{\pi}}\right)^2 \int_0^\pi \left(\int_0^\pi f\left(\frac{2n+\cos\omega_1+1}{2^{k+1}}, \frac{2n'+\cos\omega_2+1}{2^{k+1}}\right) \left(\cos(m-1)\omega_1 \right. \right. \\ &\quad \left. \left. - \cos(m+1)\omega_1\right) d\omega_1\right) \sin m'\omega_2 \sin \omega_2 d\omega_2, \\ &= \left(\frac{1}{8}\sqrt{\frac{8}{\pi}}\right) \int_0^\pi A_{n,m}(\omega_1, \omega_2) \sin m'\omega_2 \sin \omega_2 d\omega_2, \end{aligned}$$

where $A_{n,m}(\omega_1, \omega_2) = \frac{1}{8}\sqrt{\frac{8}{\pi}} \int_0^\pi f\left(\frac{2n+\cos\omega_1+1}{2^{k+1}}, \frac{2n'+\cos\omega_2+1}{2^{k+1}}\right) \left(\cos(m-1)\omega_1 - \cos(m+1)\omega_1\right) d\omega_1$.

Now,

$$A_{n,m}(\omega_1, \omega_2) = \frac{1}{8}\sqrt{\frac{8}{\pi}} \frac{1}{2^{k+1}} \int_0^\pi f_{\omega_1}\left(\frac{2n+\cos\omega_1+1}{2^{k+1}}, \frac{2n'+\cos\omega_2+1}{2^{k+1}}\right) \left(\frac{\sin(m-1)\omega_1 \sin \omega_1}{(m-1)}\right)$$

$$\begin{aligned}
& - \frac{1}{(m+1)} \int_0^\pi f_{\omega_1} \left(\frac{2n + \cos \omega_1 + 1}{2^{k+1}}, \frac{2n' + \cos \omega_2 + 1}{2^{k+1}} \right) \sin(m+1)\omega_1 \sin \omega_1 \, d\omega_1, \\
& = \frac{1}{8} \sqrt{\frac{8}{\pi}} \frac{1}{2^{k+1}} (I_1 - I_2),
\end{aligned}$$

where

$$I_1 = \frac{1}{(m-1)} \int_0^\pi f_{\omega_1} \left(\frac{2n + \cos \omega_1 + 1}{2^{k+1}}, \frac{2n' + \cos \omega_2 + 1}{2^{k+1}} \right) \sin(m-1)\omega_1 \sin \omega_1 \, d\omega_1,$$

and

$$I_2 = \frac{1}{(m+1)} \int_0^\pi f_{\omega_1} \left(\frac{2n + \cos \omega_1 + 1}{2^{k+1}}, \frac{2n' + \cos \omega_2 + 1}{2^{k+1}} \right) \sin(m+1)\omega_1 \sin \omega_1 \, d\omega_1.$$

Let us estimate the values of I_1 as

$$\begin{aligned}
I_1 &= \frac{1}{(m-1)} \int_0^\pi f_{\omega_1} \left(\frac{2n + \cos \omega_1 + 1}{2^{k+1}}, \frac{2n' + \cos \omega_2 + 1}{2^{k+1}} \right) \sin(m-1)\omega_1 \sin \omega_1 \, d\omega_1, \\
&= \frac{1}{2(m-1)} \int_0^\pi f_{\omega_1} \left(\frac{2n + \cos \omega_1 + 1}{2^{k+1}}, \frac{2n' + \cos \omega_2 + 1}{2^{k+1}} \right) (\cos(m-2)\omega_1 - \cos m\omega_1) \, d\omega_1, \\
&= \frac{2^{-k-1}}{2(m-1)} \left(\frac{1}{(m-2)} \int_0^\pi f_{\omega_1 \omega_1} \left(\frac{2n + \cos \omega_1 + 1}{2^{k+1}}, \frac{2n' + \cos \omega_2 + 1}{2^{k+1}} \right) \sin(m-2)\omega_1 \times \right. \\
&\quad \left. \sin \omega_1 \, d\omega_1 - \frac{1}{m} \int_0^\pi f_{\omega_1 \omega_1} \left(\frac{2n + \cos \omega_1 + 1}{2^{k+1}}, \frac{2n' + \cos \omega_2 + 1}{2^{k+1}} \right) \sin m\omega_1 \sin \omega_1 \, d\omega_1 \right), \\
&= \frac{2^{-k-1}}{2(m-1)} \int_0^\pi f_{\omega_1 \omega_1} \left(\frac{2n + \cos \omega_1 + 1}{2^{k+1}}, \frac{2n' + \cos \omega_2 + 1}{2^{k+1}} \right) \left(\frac{\sin(m-2)\omega_1 \sin \omega_1}{(m-2)} \right. \\
&\quad \left. - \frac{\sin m\omega_1 \sin \omega_1}{m} \right) \, d\omega_1.
\end{aligned}$$

Similarly the value of I_2 is

$$\begin{aligned}
I_2 &= \frac{2^{-k-1}}{2(m+1)} \int_0^\pi f_{\omega_1 \omega_1} \left(\frac{2n + \cos \omega_1 + 1}{2^{k+1}}, \frac{2n' + \cos \omega_2 + 1}{2^{k+1}} \right) \left(\frac{\sin m\omega_1 \sin \omega_1}{m} \right. \\
&\quad \left. - \frac{\sin(m+2)\omega_1 \sin \omega_1}{(m+2)} \right) \, d\omega_1.
\end{aligned}$$

Thus, we have

$$c_{n,m,n',m'} = \frac{1}{8} \sqrt{\frac{8}{\pi}} \times \frac{2^{-2k-2}}{\sqrt{8\pi}} \int_0^\pi \int_0^\pi f_{\omega_1\omega_1} \left(\frac{2n + \cos \omega_1 + 1}{2^{k+1}}, \frac{2n' + \cos \omega_2 + 1}{2^{k+1}} \right) \sin m' \omega_2 \sin \omega_2 \\ \times d\omega_2 \Omega_1(\omega_1) d\omega_1,$$

where

$$\Omega_1(\omega_1) = \left[\frac{1}{2(m-1)} \left(\frac{\sin(m-2)\omega_1 \sin \omega_1}{(m-2)} - \frac{\sin m\omega_1 \sin \omega_1}{m} \right) - \frac{1}{2(m+1)} \left(\frac{\sin m\omega_1 \sin \omega_1}{m} \right. \right. \\ \left. \left. - \frac{\sin(m+2)\omega_1 \sin \omega_1}{(m+2)} \right) \right],$$

Now integrating twice w.r. to ω_2 , we get

$$c_{n,m,n',m'} = \frac{2^{-4k-4}}{8\pi} \int_0^\pi \int_0^\pi f_{\omega_1\omega_1\omega_2\omega_2} \left(\frac{2n + \cos \omega_1 + 1}{2^{k+1}}, \frac{2n' + \cos \omega_2 + 1}{2^{k+1}} \right) \Omega_1(\omega_1) \Omega_2(\omega_2) d\omega_1 d\omega_2,$$

where

$$\Omega_2(\omega_2) = \left[\frac{1}{2(m'-1)} \left(\frac{\sin(m'-2)\omega_2 \sin \omega_2}{(m'-2)} - \frac{\sin m'\omega_2 \sin \omega_2}{m'} \right) - \frac{1}{2(m'+1)} \right. \\ \left. \left(\frac{\sin m'\omega_2 \sin \omega_2}{m'} - \frac{\sin(m'+2)\omega_2 \sin \omega_2}{(m'+2)} \right) \right],$$

or

$$|c_{n,m,n',m'}| = \left| \frac{2^{-4k-4}}{8\pi} \int_0^\pi \int_0^\pi f_{\omega_1\omega_1\omega_2\omega_2} \left(\frac{2n + \cos \omega_1 + 1}{2^{k+1}}, \frac{2n' + \cos \omega_2 + 1}{2^{k+1}} \right) \Omega_1(\omega_1) \right. \\ \left. \Omega_2(\omega_2) d\omega_1 d\omega_2 \right|,$$

$$|c_{n,m,n',m'}| \leq \frac{2^{-4k-4} B}{8\pi} \int_0^\pi \int_0^\pi |\Omega_1(\omega_1) \Omega_2(\omega_2)| d\omega_1 d\omega_2.$$

After some mathematical calculations, we get

$$|c_{n,m,n',m'}| < \frac{9\pi}{32} \frac{B}{(n+1)^2(m-2)^4(n'+1)^2(m'-2)^4}, \quad m > 2, \quad m' > 2.$$

This completes the proof. \square

Proof. (ii)

$$\begin{aligned} \sigma_{f,k,M}^2 &= \int_0^1 \int_0^1 \left[f(x,y) - \sum_{n=0}^{2^k-1} \sum_{m=1}^M \sum_{n'=0}^{2^k-1} \sum_{m'=1}^M c_{n,m,n',m'} \psi_{n,m}(x) \psi_{n',m'}(y) \right]^2 \omega_n(x) \omega'_n(y) dx dy, \\ &= \int_0^1 \int_0^1 \left| \sum_{n=2^k}^{\infty} \sum_{m=1+M}^{\infty} \sum_{n'=2^k}^{\infty} \sum_{m'=1+M}^{\infty} c_{n,m,n',m'} \psi_{n,m}(x) \right|^2 \omega_n(x) \omega_n(y) dx dy, \\ &= \sum_{n=2^k}^{\infty} \sum_{m=1+M}^{\infty} \sum_{n'=2^k}^{\infty} \sum_{m'=1+M}^{\infty} |c_{n,m,n',m'}|^2, \end{aligned}$$

$$\sigma_{f,k,M}^2 < \frac{9\pi}{32} \sum_{n=2^k}^{\infty} \sum_{m=M+1}^{\infty} \sum_{n'=2^k}^{\infty} \sum_{m'=M+1}^{\infty} \frac{B}{(1+n)^2(m-2)^4(1+n')^2(m'-2)^4}.$$

Hence the proof is completed. \square

4.7 Numerical results

To illustrate the absolute error at (x_i, t_j) , the following notation is adopted in order to demonstrate it

$$e_u(x_i, t_j) = \left| u(x_i, t_j) - u_{\hat{m}}(x_i, t_j) \right|, \quad 0 \leq x_i, t_j \leq 1, \quad (4.111)$$

where $u(x_i, t_j)$ and $u_{\hat{m}}(x_i, t_j)$ are exact and approximate solutions, respectively at (x_i, t_j) .

Example 4.1 Consider the model (4.1) by assuming $d_1 = d_2 = d_3 = 0.001$, $a = 0.01$, $b = 0.01$ and $c = 0.01$ with

$$f_1(x, t) = d_1 t^2 \sin(x) + \frac{2t^{(2-\alpha)} \sin(x)}{(2 - 3\alpha + \alpha^2)\Gamma(1 - \alpha)} - t^6 \cos(x) \sin^2(x) + t^2(b + \exp(-x)t^3) \sin(x) - a,$$

$$f_2(x, t) = d_2 t^2 \cos(x) + \frac{2t^{(2-\alpha)} \cos(x)}{(2 - 3\alpha + \alpha^2)\Gamma(1 - \alpha)} - \exp(-x)t^5 \sin(x) + t^6 \cos(x) \sin^2(x),$$

$$f_3(x, t) = -c - d_3 \exp(-x)t^3 - \frac{6 \exp(-x)t^{(3-\alpha)}}{(-6 + 11\alpha - 6\alpha^2 + \alpha^3)\Gamma(1 - \alpha)} + \exp(-x)t^5 \sin(x).$$

The IC and BC's are obtained using the exact solutions $u(x, t) = t^2 \sin(x)$, $v(x, t) = t^2 \cos(x)$ and $w(x, t) = \exp(-x)t^3$.

TABLE 4.1: Tabular presentation of absolute errors for different values of α at $t = 0.5$ and $\hat{m} = 12$ for Example 4.1

α	x	$e_u(x, t)$	$e_v(x, t)$	$e_w(x, t)$
0.50	0.2	1.2766×10^{-07}	5.5915×10^{-07}	3.7332×10^{-09}
	0.4	2.4041×10^{-07}	5.2467×10^{-07}	1.1687×10^{-08}
	0.6	3.3862×10^{-07}	4.9282×10^{-07}	1.4846×10^{-08}
	0.8	4.5241×10^{-07}	4.2715×10^{-06}	3.1818×10^{-07}
	1.0	4.9127×10^{-15}	4.4964×10^{-15}	5.5511×10^{-17}
0.55	0.2	3.9620×10^{-08}	2.9657×10^{-07}	6.2746×10^{-08}
	0.4	9.1724×10^{-08}	2.7611×10^{-07}	6.3076×10^{-08}
	0.6	1.4732×10^{-07}	2.1576×10^{-07}	5.9016×10^{-08}
	0.8	3.1039×10^{-08}	3.3590×10^{-06}	8.3650×10^{-07}
	1.0	7.7438×10^{-15}	1.1102×10^{-15}	8.8124×10^{-16}

Table 4.1 is designed for the absolute errors of Example 4.1, for two different values of fractional order $\alpha = 0.50$ and $\alpha = 0.55$ at $\hat{m} = 12$. It is seen from the table that the results obtained from the proposed method are very closed to the exact solutions even for small value of approximation \hat{m} and thus the proposed approach in this research is accurate and effective not only to solve the FPDE but also to solve

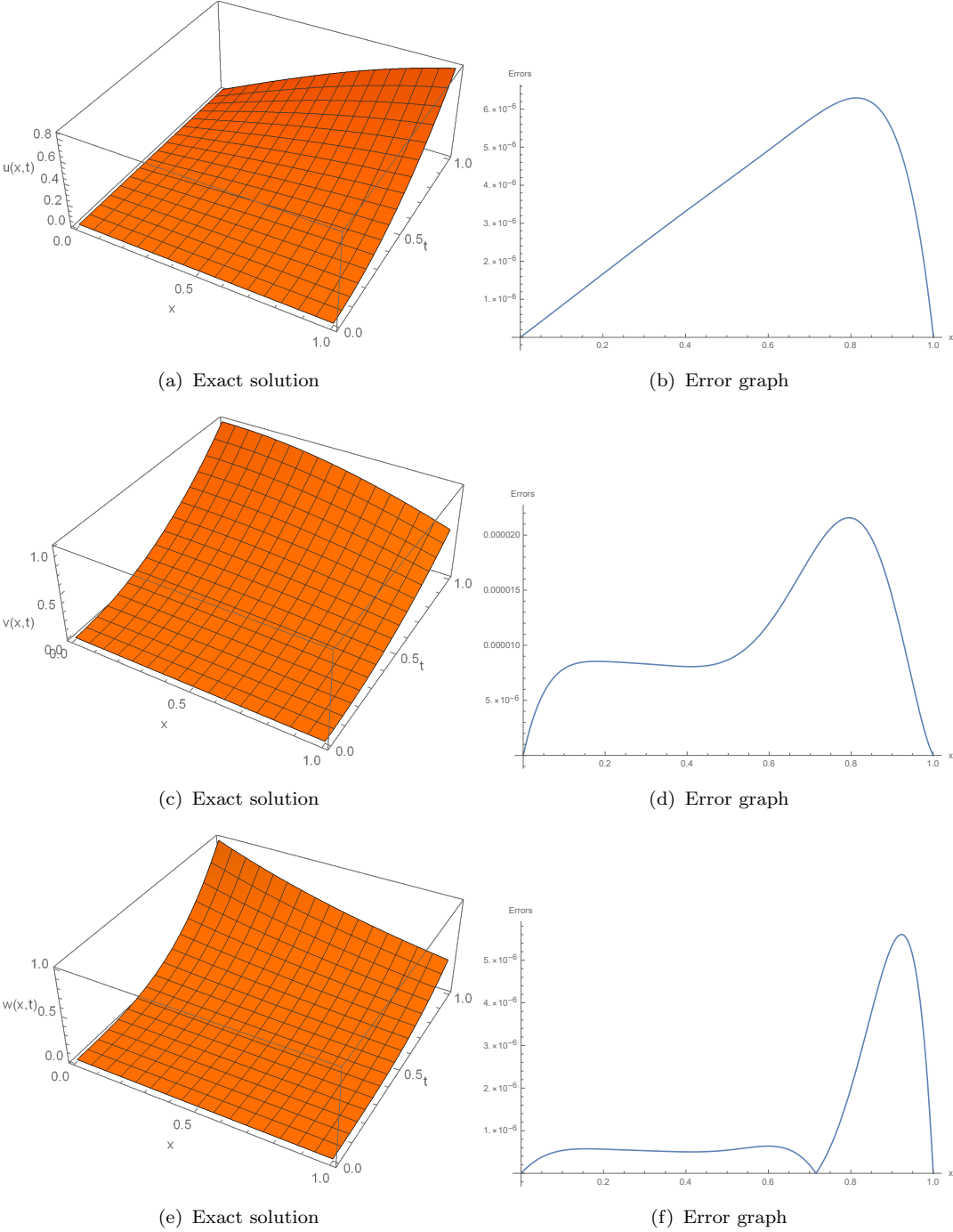


FIGURE 4.1: Behaviour of exact solutions and their corresponding Error graph at $t = 0.5$ for Example 4.1 at $\hat{m} = 9$.

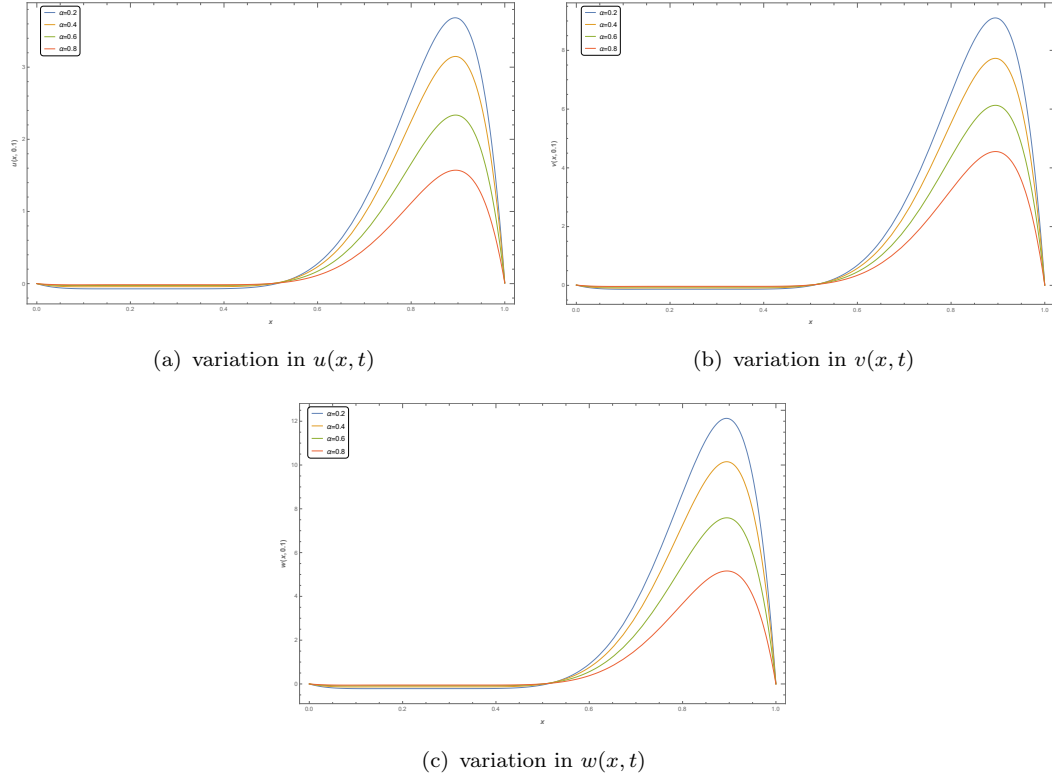


FIGURE 4.2: Graph for the variation in concentrations for different values of α at $t = 0.1$ for Example 4.1 at $\hat{m} = 8$.

the system of FPDEs. Fig 4.1 is plotted to show the behaviour of exact solutions and their corresponding absolute errors obtained by the proposed technique, while behaviour of concentrations for various values of α ($0 < \alpha \leq 1$) at $t = 0.1$ with $f_1(x, t) = -0.1$, $f_2(x, t) = -0.2$ and $f_3(x, t) = -0.3$ are shown through Fig 4.2.

Example 4.2 By assuming $d_1 = d_2 = d_3 = 1$, $a = 0.125$, $b = 0.250$ and $c = 0.001$, the model (4.1) reduces to

$$\begin{aligned}\frac{\partial^\alpha u}{\partial t^\alpha} &= \frac{\partial^2 u}{\partial x^2} + 0.125 - (0.250 + w)u + u^2 v + f_1(x, t), \\ \frac{\partial^\alpha v}{\partial t^\alpha} &= \frac{\partial^2 v}{\partial x^2} + uw - u^2 v + f_2(x, t), \\ \frac{\partial^\alpha w}{\partial t^\alpha} &= \frac{\partial^2 w}{\partial x^2} - uw + 0.001 + f_3(x, t),\end{aligned}$$

where $f_i(x, t)$, $i = 1, 2, 3$, IC and BC's can be determined with the exact solutions

$u(x, t) = (x t(1 - x))^2(1 - t)^3$, $v(x, t) = x^2(1 - x) \exp(-t)$ and $w(x, t) = t^2 \cosh(x)$.

TABLE 4.2: Tabular presentation of absolute errors for different values of \hat{m} at $\alpha = 0.73$ and $t = 0.5$ for Example 4.2

\hat{m}	x	$e_u(x, t)$	$e_v(x, t)$	$e_w(x, t)$
08	0.2	2.9342×10^{-07}	8.6525×10^{-06}	5.2077×10^{-06}
	0.4	4.7976×10^{-07}	1.3022×10^{-05}	8.8786×10^{-06}
	0.6	5.0402×10^{-07}	1.2133×10^{-05}	9.3533×10^{-06}
	0.8	3.7805×10^{-07}	7.2176×10^{-06}	6.3683×10^{-06}
	1.0	1.6252×10^{-14}	2.6371×10^{-13}	3.1019×10^{-12}
12	0.2	3.1091×10^{-08}	2.2588×10^{-06}	7.4312×10^{-07}
	0.4	5.2793×10^{-08}	4.1730×10^{-06}	1.1248×10^{-06}
	0.6	5.2761×10^{-08}	4.8133×10^{-06}	1.1715×10^{-06}
	0.8	1.4438×10^{-07}	5.5305×10^{-06}	3.9073×10^{-07}
	1.0	1.7588×10^{-17}	5.7404×10^{-16}	1.6819×10^{-14}

The absolute error between exact solution and numerical solution obtained using the proposed method for Example 4.2, are depicted in Table 4.2. This Example 4.2 is solved for the fractional order $\alpha = 0.73$ for two different values of $\hat{m} = 8$ and $\hat{m} = 12$. From Table 4.2, it is observed that on increasing the number of approximations, the errors are decreasing. Graphical presentations of Exact solutions and their corresponding absolute errors can be seen in Fig 4.3. The variations in the values of concentrations for different values of α at $t = 0.1$ with $f_1(x, t) = -0.1$, $f_2(x, t) = 2$ and $f_3(x, t) = 0$ have been demonstrated in Fig 4.4.

Example 4.3 Consider the following time fractional reaction-diffusion equation

$$\frac{\partial^\alpha u}{\partial t^\alpha} = \frac{\partial^2 u}{\partial x^2} - u(x, t) + f(x, t),$$

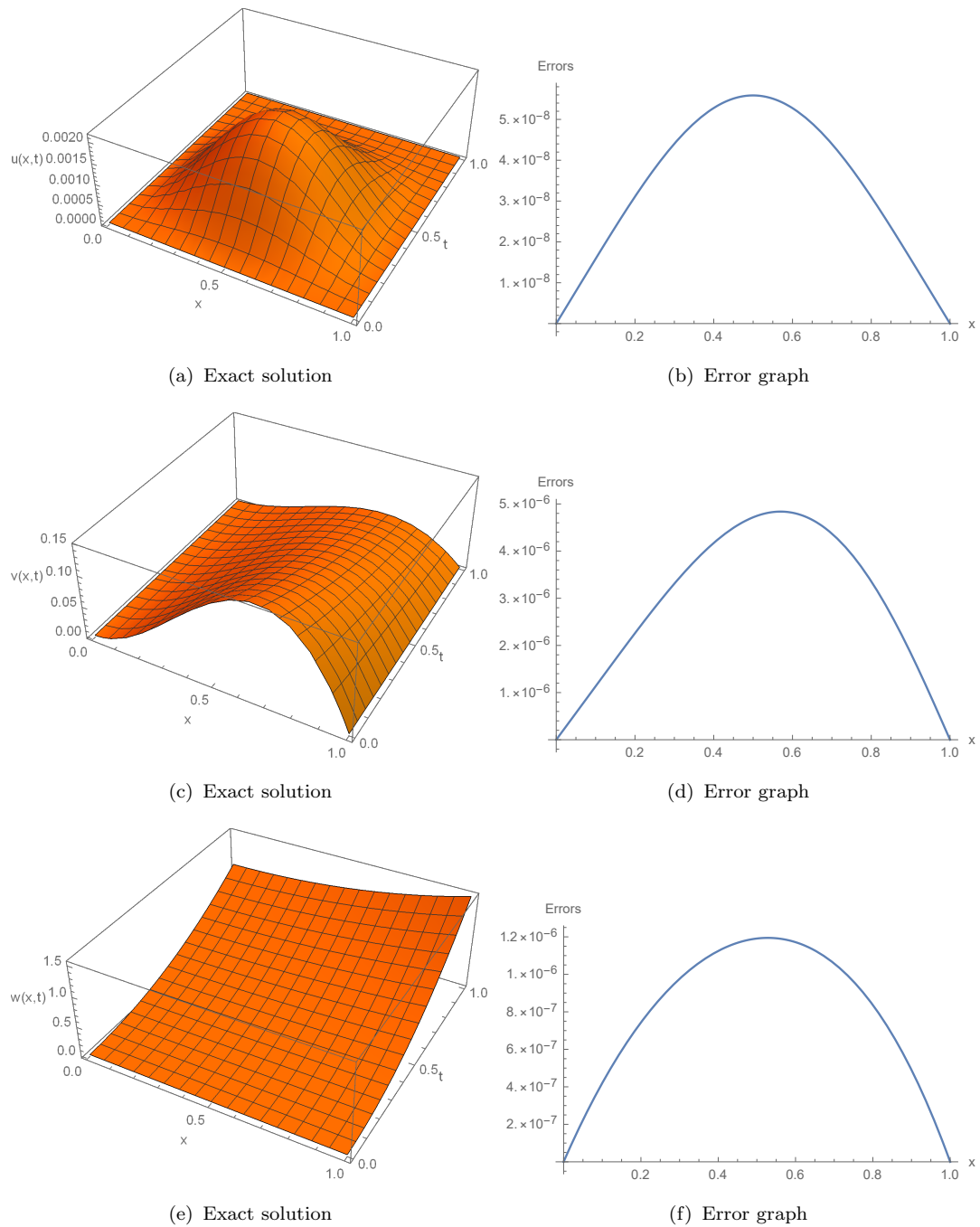


FIGURE 4.3: Behaviour of exact solutions and their corresponding Error graphs at $t = 0.5$ for Example 4.2 at $\hat{m} = 12$.

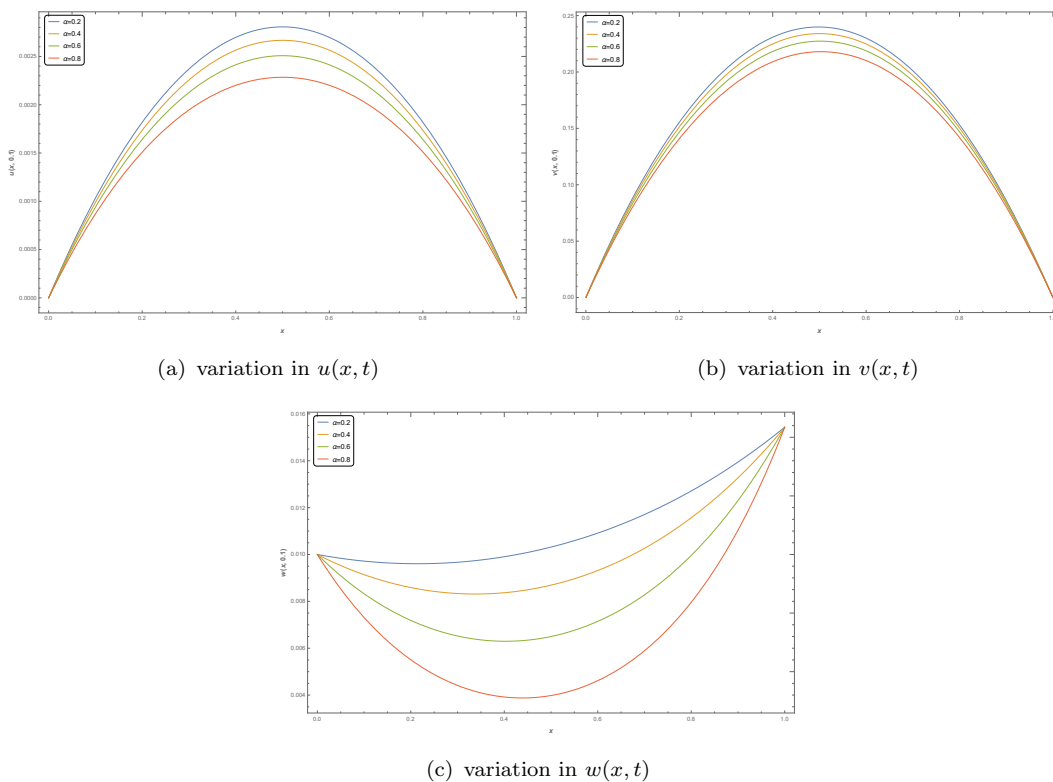


FIGURE 4.4: Graph for the variation in concentrations for different values of α at $t = 0.1$ for Example 4.2 at $\hat{m} = 8$.

under the following initial and boundary conditions

$$u(x, 0) = 0,$$

$$u(0, t) = u(2, t) = 0,$$

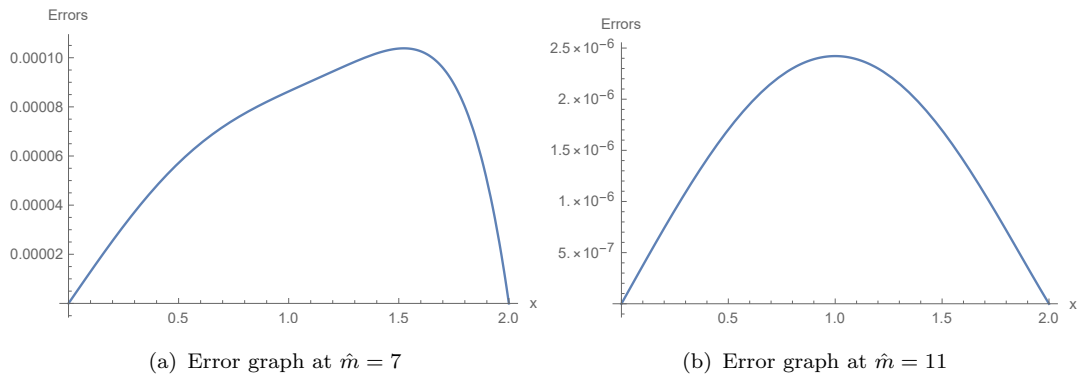
and

$$f(x, t) = \frac{2t^{2-\alpha}}{\Gamma(3-\alpha)}x(2-x) + t^2x(2-x) + 2t^2,$$

with the exact solution as $u(x, t) = t^2x(2-x)$.

TABLE 4.3: Comparison of exact and numerical solution at $\alpha = 0.70$ and $t = 0.4$ for Example 4.3

x	0.4	0.8	1.2	1.6
Exact solution	0.102400	0.153600	0.153600	0.102400
Implicit scheme	0.102396	0.153750	0.153750	0.102396
E-I scheme[121]	0.102526	0.153343	0.153343	0.102526
I-E scheme[121]	0.102522	0.153580	0.153580	0.102522
PASE-I scheme[122]	0.102339	0.153288	0.153288	0.102339
PASI-E scheme[122]	0.102474	0.153262	0.153613	0.102356
Present method	0.102398	0.153597	0.153597	0.102398

FIGURE 4.5: Variations in errors for different values of \hat{m} at $t = 0.5$ and $\alpha = 0.70$ for Example 4.3.

Here the numerical solution obtained by the proposed method is compared with the schemes in [121, 122]. To obtain the numerical solution, Example 4.3 is solved for $\hat{m} = 11$, and the results are depicted in Table 4.3. From the table, it can be seen that the numerical results obtained by the presented method are performing well as compared to the existing schemes in [121, 122] and are very closed to the exact solution. The absolute error graphs of Example 4.3 for two different values of \hat{m} are shown in Fig 4.5, which are designed to show that as the number of approximation increases, the error decreases rapidly.

4.8 Conclusion

This chapter successfully introduces and applies the Vieta-Fibonacci wavelet and collocation method for solving numerically the three-component time fractional order Brusselator reaction-diffusion system, by deriving operational matrices for both integer and fractional order derivatives. The uniqueness and existence of the solution for the considered model are discussed. Also the Ulam-Hyers stability of fractional order has been considered. Moreover, the comprehensive convergence analysis highlights the effectiveness of the Vieta-Fibonacci wavelet method. The ability of the method yields accurate results while significantly reducing computational complexity makes it a valuable addition to the field of computational mathematics. By bridging the gap between the Vieta-Fibonacci wavelet method and fractional-order reaction-diffusion system, this study advances the understanding of complex phenomena in diverse domains, including chemical kinetics, biology, and physics. The applicability of this approach holds promise for addressing the real-world problems those involve fractional-order differential equations.
